An Improved Wind Driven Optimization Algorithm for Parameters Identification of a Triple-Diode Photovoltaic Cell Model

Ibrahim Anwar Ibrahim[1], M. J. Hossain[2], Benjamin C. Duck[3], Mithulananthan Nadarajah[4]

[1]School of Engineering, Macquarie University, Sydney, NSW 2109, Australia

[2]School of Electrical and Data Engineering, University of Technology Sydney, Sydney, NSW 2007, Australia

[3]CSIRO Energy, 10 Murray Dwyer Cct, Mayfield West, NSW 2304, Australia

[4] School of Information Technology and Electrical Engineering, The University of Queensland, Brisbane, QLD 4072, Australia

[1]ibrahim.a.ibrahim@hdr.mq.edu.au ; [1]ibrahim.a.ibrahim@ieee.org ; [2]jahangir.hossain@uts.edu.au ; [3]benjamin.duck@csiro.au ; [4]mithulan@itee.uq.edu.au

Abstract

The double-diode photovoltaic (PV) cell model is insufficient to accurately characterize the different current components of a PV cell. Therefore, the triple-diode model of a PV cell is considered to model its complicated physical characteristics by clearly defining the different current components of the PV cell. The identification of its unknown parameters is a complex, multi-modal and multi-variable optimization problem. An improved wind driven optimization (IWDO) algorithm is proposed in this paper to identify its nine unknown parameters. The proposed method is a combination of the mutation strategy of the differential evolution (DE) algorithm and the covariance matrix adaptation evolution strategy (CMAES) of the wind driven optimization (WDO) algorithm. The mutation strategy aims to bolster the exploration ability of the IWDO algorithm, while the CMAES based WDO algorithm aims to improve the searching of the classical WDO algorithm. Therefore, IWDO algorithm is more accurate and faster than the classical WDO algorithm in finding the global optimum and balancing exploration and exploitation. The proposed model has been utilized on 15-minute interval data to identify the unknown parameters of three commercial PV modules, namely: mono-crystalline LG300N1C-A3, poly-crystalline JAP6-60-250W/3BB and thin-film Avancis PowerMax smart 125W. To show the effectiveness of the proposed model, its performance is validated by comparing it with that obtained by the classical WDO, the adaptive wind driven optimization (AWDO), moth-flame optimizer (MFO), sunflower optimization (SFO) and the improved opposition-based whale optimization (IOWO) algorithms. The results demonstrate that IWDO outperforms the aforementioned models in accuracy, convergence speed and feasibility. In addition, IWDO more clearly defined different current components and generated any current-voltage (I-V) curve under any operating condition.

Keywords: Photovoltaic (PV); triple-diode model; parameter identification; I-V characteristic curve; IWDO algorithm.

Nomenclature

Abbreviations

I-V	current-voltage
P-V	power-voltage
RMSE	root-mean-square-error
PSO	particle swarm optimization
MFO	moth-flame optimizer
SFO	sunflower optimization
IOWO	improved opposition-based whale optimization
CPSO	chaos particle swarm optimization
ELPSO	enhanced leader particle swarm optimization
TVACPSO	time varying acceleration coefficients particle swarm optimization
MPSO	mutated particle swarm optimization
GCPSO	guaranteed convergence particle swarm optimization
ABC	artificial bee colony
MABC	modified artificial bee colony
DE	differential evolution
IADE	improved adaptive differential evolution
BBO	biogeography-based optimization
BBO-M	biogeography-based optimization algorithm with mutation strategies
GOTLBO	generalised opposition-based teaching learning-based optimization
WDO	wind driven optimization
BPFPA	bee pollinator flower pollination algorithm
FPA	flower pollination algorithm
CSO	cat swarm optimization
CWOA	chaotic whale optimization algorithm
SATLO	self-adaptive teaching learning-based optimization
AWDO	adaptive wind driven optimization
CMAES	covariance matrix adaptation evolution strategy
BFO	bacterial foraging optimization
IWDO	improved wind driven optimization
KCL	Kirchhoff's current law
KVL	Kirchhoff's voltage law
NAvg	normal average
SD	standard deviation
nRMSE	normalized root-mean-square error
MAPE	mean absolute percentage error
R^2	coefficient of determination
CSIRO	Commonwealth Scientific and Industrial Research Organisation
NSW	New South Wales
DBSCAN	density-based spatial clustering of applications with noise
s.	second

Symbols

I	the output current of the PV cell
I_{Ph}	the generated photocurrent
I_{0_1}	the first diode reverse saturation current
I_{0_2}	the second diode reverse saturation current
I_{0_3}	the third diode reverse saturation current
V	the voltage output of the PV cell

R_s	the series resistance
R_{sh}	the shunt resistance
V_{t_1}	the first diode' thermal voltage
V_{t_2}	the second diode' thermal voltage
V_{t_3}	the third diode' thermal voltage
a_1	the ideality factor of the first diode
a_2	the ideality factor of the second diode
a_3	the ideality factor of the third diode
k_b	Boltzmann's constant
q	the electron's charge
T_c	the cell temperature (K)
V_a	the actual PV module output voltage
I_a	the actual PV module output current
I_e	the estimated PV module output current
θ	the vector of the nine unknown parameters (i.e., I_{Ph}, I_{0_1}, I_{0_2}, I_{0_3}, a_1, a_2, a_3, R_s and R_{sh})
N	the length of the experimental database
$\overrightarrow{F_t}$	a vector of the total forces on an air parcel
ρ	the density of the air parcel
$\vec{a}$	the acceleration vector
D_j	the dimensions of the optimization problem
j	the number of unknown parameters
N_k	the population size of the air parcels
k	the population
$Upper_j$	the upper limit for each D_j
$Lower_j$	the lower limit for each D_j
G_{max}	the maximum number of iterations
u_{max}	the maximum allowable limit of the velocity for the air parcels
$\overrightarrow{y_{N_J}^k}$	the position vector
$\overrightarrow{u_{N_J}^k}$	the velocity vector
$\overrightarrow{u_{new_J}^k}$	the air parcel's new velocity vector
$\overrightarrow{y_{new_J}^k}$	the air parcel's new position vector
$u_{c_{j-1}}^k$	the air parcel's velocity at the current iteration
$y_{c_{j-1}}^k$	the air parcel's position at the current iteration
$y_{opt_j}^k$	the air parcel's optimal position
r^k	the ranking among all air parcels
G	the current iteration
$Vec_{i,G}$	the mutant vector
$Z_{i,G}$	the individual in the current air parcel population
r_1^i	the first mutually exclusive integer which is generated within the range from 1 to N_k randomly
r_2^i	the second mutually exclusive integer which is generated within the range from 1 to N_k randomly
$Z_{best,G}$	the best individual with the best fitness function value in k at G
F	the scale factor which is a positive control parameter that aims to scale the difference vector
X_i	the parent
U_i	the offspring

μ_j	the upper limit of the ith dimension in the mutation strategy
δ_j	the lower limit of the ith dimension in the mutation strategy
$Z_i(j)$	the individual in the current air parcel
$rndreal(0,1)$	a random number between 0 and 1
$f(U_i, G)$	the objective function values based on the mutation phase
$f(X_i, G)$	the objective function values based on the ranking of air parcels
$Parameter_i$	the value for each identified parameter
$\overline{Parameter}$	the mean value of each identified parameter
M	the length of the vector of each identified parameter
I_c	the calculated PV output current based on the Newton-Raphson method
Var	the variance

1. Introduction

Renewable sources can overcome the challenges of conventional fossil fuel-based power sources due to the latter's increasing cost, their problematic depletion, and negative impacts on the environment and its societies. Solar energy has gained momentum as one of the finest energy resources. At present, it is the third most widely used source of electrical energy in most continental regions due to broad availability, high visibility, safe use, and range of applications for residential, commercial and utility users alike. A photovoltaic (PV) system is one of the most direct way to provide the electrical energy from the solar energy based on the inherent properties of semiconductors [1].

Accurate modeling of PV system is crucial to maximize its energy harvesting. The current-voltage (I-V) and power-voltage (P-V) curves are very useful representations to model the non-linear characteristic of the PV cell/module based on the variation of meteorological variables. They can be derived by utilizing the parameters of the diode PV cell model which are considered as a direct indicator of the PV modules' performance [2]. The unknown parameters of PV cell models are identified from experimental data in a reverse process. This process is still a challenge for researchers as it strongly depends on several non-linear relationships which govern the PV cell/module behaviour [3]. In literature, several models are proposed to characterize the I-V curves of PV cells which are the single-diode [3], the double-diode [4], the modified double-diode [5] and the triple-diode [6] PV cell models. Selecting the proper model depends on the application and understanding the trade-off between model simplicity and model accuracy. The increasing installations of large PV scale projects require accurate characterizing models, especially at low solar radiation conditions for designing control schemes for integrating PV systems to ensure the stability of power systems. Therefore, the triple-diode PV cell model is more accurate than other diode PV cell models as it considers the impact of the leakage current, the carrier recombination and the grain boundaries [7].

The identification of the unknown parameters is the most used and useful approach to characterize the non-linear behaviour of PV cells. This approach can be considered as an optimization problem which is known as a PV parameter identification problem. The unknown parameters are identified in subject to minimize the root-mean-square-error (RMSE) value between the obtained and actual measured

currents. The availability of the information and the type of the identification method affect the accuracy of the PV cell model. The availability of the information guides to understand how the identified parameters can perform the characteristic of the mathematical model. The unknown parameters can be determined from the datasheets of the manufacturer [8] or the actual recorded I-V characteristic curves [3]. Generally, two classes of approaches are usually utilized to resolve the PV cell/module parameter identification problem, namely, deterministic and heuristic approaches [9]. Deterministic approaches are used widely to identify the unknown parameters. Deterministic approaches are again divided into iterative or analytical methods. The iterative methods include but are not limited to the Levenberg-Marquardt and the Newton-Raphson methods. The solutions based on these methods are dependent on the initial parameters and mostly they are trapped into local optima. In addition, iterative methods need many iterations to scan all the probabilities in the search space which requires long computational time. In contrast, analytical methods are fast, but they need simplifications and assumptions to determine the unknown parameters due to the multi-variability and non-linearity of the identification problem [10]. Due to the shortcomings of iterative and analytical methods, deterministic approaches are not suitable to identify the PV cell parameters. Heuristic approaches are proposed to find the optimal unknown parameters based on global optimization population algorithms. Heuristic approaches have several advantages over deterministic approaches. Primarily, they do not have any restriction on the problem formulation, the simplicity in the conceptual and computational optimization procedure and their ability to handle multi-modal optimization problems [11]. Many heuristic approaches have been successfully utilized for identifying the PV cell parameters in the past decade. For example, the particle swarm optimization (PSO) [12], moth-flame optimizer (MFO) [7] and sunflower optimization (SFO) algorithms [13] have been used to identify the triple-diode PV cell model's parameters. The results obtained by PSO, MFO and SFO algorithms are inconsistent as different results can be obtained by repeating the optimization process. Moreover, these algorithms need more iterations to secure the convergence of the optimization problem. To overcome these challenges, some improved algorithms are proposed in the literature such as the improved opposition-based whale optimization (IOWO) algorithm [6]. Here, the classical heuristic approaches need improvements to reduce the number of iteration and to guarantee consistent results with an effective convergency.

Several improved heuristic approaches are proposed in the literature [14] such as the chaos particle swarm optimization (CPSO) [15], enhanced leader particle swarm optimization (ELPSO) [16], time varying acceleration coefficients particle swarm optimization (TVACPSO) [17], mutated particle swarm optimization (MPSO) [18], guaranteed convergence particle swarm optimization (GCPSO) [19], modified artificial bee colony (MABC) [20], improved adaptive differential evolution (IADE) [21], biogeography-based optimization algorithm with mutation strategies (BBO-M) [22] and generalised opposition-based teaching learning-based optimization (GOTLBO) [23] algorithms. The aforementioned algorithms have some demerits. Variants of PSO algorithm such CPSO, ELPSO,

TVACPSO, MPSO and GCPSO are adaptive PSO algorithms which overcome the limitations of the classical PSO effectively in both convergence and finding global optima. The demerit of such algorithms is that they require tuning of four or more parameters, which complete the control of these parameters as well as increase the computational time. MABC algorithm needs relatively a large population size to reduced computational time. IADE algorithm is proposed to address the challenges of the classical differential evolution (DE) algorithm. However, several parameters of the IADE algorithm should be adjusted which increases the computational time. BBO-M algorithm requires relatively a larger population size to minimize its computational time comparing with the classical biogeography-based optimization (BBO) algorithm. GOTLBO is carried out based on opposition-based learning which enhances the explorative capability and convergency. On the other hand, this algorithm cannot exploit solutions effectively, meaning it may struggle to acquire the optimum solution.

The wind driven optimization (WDO) algorithm is proposed by Bayraktar et al. [24] to solve the optimization problems which is inspired from the wind movements on the Earth. The WDO algorithm has several merits among other heuristic algorithms, for example (i) its solutions are built from random operations to avoid being stuck in local optima; (ii) its robustness in parameter interdependency; and (iii) the capability of dealing with high multi-modal problems.

Several studies of WDO algorithm have been addressed in the literature in two categories: (i) using the WDO algorithm to solve the optimization problems; and (ii) improving its performance. Mathew et al. [4] used the WDO algorithm to identify the parameters of a double-diode PV cell model which yielded better results than those obtained by the bee pollinator flower pollination algorithm (BPFPA), flower pollination algorithm (FPA), cat swarm optimization (CSO), chaotic whale optimization algorithm (CWOA) and self-adaptive teaching learning-based optimization (SATLO) algorithms. In addition, Bayraktar and Komurcu [25] improved the classical WDO algorithm, which is called the adaptive wind driven optimization (AWDO) algorithm, by integrating the covariance matrix adaptation evolution strategy (CMAES) to tune the hyper-parameters of WDO algorithm thereby enhancing convergence speed. Accordingly, Ibrahim et al. [26] applied the AWDO algorithm to identify the single-diode PV cell model's parameters. The results demonstrated the superior performance of the proposed algorithm over the bacterial foraging optimization (BFO), BBO and PSO algorithms.

One of the main drawbacks of WDO algorithm is that its speed and accuracy when exploring the search space are relatively low. To address this drawback and other limitations of the aforementioned algorithms, an improved wind driven optimization (IWDO) algorithm is proposed. This algorithm is integrating the mutation strategy of the DE algorithm, which has fast and accurate exploration ability, with the classical WDO algorithm based on CMAES to enhance the searching of the classical WDO to find the global optimum whilst balancing exploration and exploitation.

In this paper, the IWDO algorithm is proposed and applied to identify the triple-diode PV cell model's parameters. To validate the proposed algorithm, IWDO algorithm is applied on three different PV model technologies, i.e. mono-crystalline, poly-crystalline and thin-film. Subsequently, its accuracy is compared with that resulted by the WDO, AWDO, MFO [7], SFO [13] and IOWO [6] algorithms. The merits of the IWDO model are given below:

- The IWDO algorithm improves the ability of finding the global optimum and balancing the exploration and exploitation by integrating the mutation strategy and CMAE strategy in the classical WDO algorithm.
- It has better accuracy and convergence speed comparing with the classical WDO and AWDO algorithms, especially in identifying the triple-diode PV cell model's parameters.
- It can handle any I-V characteristic curve of mono-crystalline, poly-crystalline and thin-film PV technologies under any operating condition based on 15-minute intervals.

The rest of this paper is organized as follows. The mathematical model of a triple-diode PV cell model and the problem formulation are described in Section 1. Section 2 describes the IWDO algorithm. Section 3 proposes the unknown parameter identification method and its flowchart in detail. In Section 4, the obtained results, validation and comparison study are presented. Section 5 summarizes the main findings of this paper.

2. Triple-diode Photovoltaic Cell Model Description and Problem Formulation

The triple-diode PV cell model is considered a more precise model than the ideal, single and double-diode PV cell models by meeting the relatively complicated non-linear behaviour of the PV cell. In fact, the triple-diode PV cell model can be considered as a useful model for characterizing the behaviour of the small size PV cells which is fitting for some applications where a non-negligible leakage current through peripheries occurs [27]. Thus, a third diode is included in parallel with the double-diode PV cell model (visualized in Figure 1). The main merit of this model lies in the accuracy. This model is considered as more accurate than the ideal, single-diode and double-diode PV cell models as it considered the grain boundaries influence and the large leakage current

By applying Kirchhoff's current law (KCL) and Kirchhoff's voltage law (KVL), the output current of the triple-diode PV cell model can be represented as [7]:

$$I = I_{Ph} - I_{0_1}\left(exp\left(\frac{V+IR_S}{V_{t_1}}\right)-1\right) - I_{0_2}\left(exp\left(\frac{V+IR_S}{V_{t_2}}\right)-1\right) - I_{0_3}\left(exp\left(\frac{V+IR_S}{V_{t_3}}\right)-1\right) - \frac{V+R_SI}{R_{sh}} \quad (1)$$

where V_{t_1}, V_{t_2} and V_{t_3} can be formulated as:

$$V_{t_1} = \frac{a_1 k_b T_c}{q} \quad (2)$$

$$V_{t_2} = \frac{a_2 k_b T_c}{q} \quad (3)$$

$$V_{t_3} = \frac{a_3 k_b T_c}{q} \quad (4)$$

The behaviour of a PV cell can be characterized based on I-V and P-V curves. The accurate model of the PV modules aims to ensure the minimum difference between the actual data and the calculated data under various meteorological conditions. To do so, the PV cell model's parameters should be identified optimally. To characterize the performance of the triple-diode PV cell model, nine unknown parameters should be identified. Theses parameters are $I_{Ph}, I_{0_1}, I_{0_2}, I_{0_3}, a_1, a_2, a_3, R_s$ and R_{sh}. These parameters are sensitive to the variation of meteorological variables. Therefore, actual data must be used to maintain the real characteristics of PV modules. Here, the IWDO algorithm is proposed to identify the triple-diode PV cell model's parameters. The objective function of the IWDO algorithm aims to minimize the value of the RMSE, which can be mathematically represented as follows:

$$f(\theta) = \sqrt{\frac{1}{N}\sum_{i=1}^{N} P(V_a, I_a, \theta)^2} \quad (5)$$

$$P(V_a, I_a, \theta) = I_a - I_{Ph} + I_{0_1}\left(exp\left(\frac{V + I_e R_s}{V_{t_1}}\right) - 1\right) + I_{0_2}\left(exp\left(\frac{V + I_e R_s}{V_{t_2}}\right) - 1\right) + I_{0_3}\left(exp\left(\frac{V + I_e R_s}{V_{t_3}}\right) - 1\right) + \frac{V + R_s I_e}{R_{sh}} \quad (6)$$

where V_{t_1}, V_{t_2} and V_{t_3} are given in (2), (3) and (4), respectively.

3. Improved Wind Driven Optimization Algorithm

The IWDO algorithm is proposed and implemented to improve the exploration ability and address the premature convergence of the classical WDO algorithm. The proposed algorithm employs two main strategies: (i) the CMAES to optimize the hyper-parameters of the classical WDO algorithm, which is used in the AWDO algorithm [25]; and (ii) the mutation of the DE algorithm [28] to enhance the searching capability of the classical WDO algorithm in finding the global optimum and balancing the exploration and exploitation.

The classical WDO is proposed, in 2010, by Bayraktar et al. [24], which is inspired by the horizontal air movements on the Earth. This phenomenon is called wind. Wind moves from the high-pressure regions to the low-pressure regions based on temperature difference. The forces which affect the movements of a parcel of air are mathematically formulated by Newton's second law of motion as [29]:

$$\rho . \vec{a} = \sum \overrightarrow{F_t} \quad (7)$$

The classical WDO algorithm has four hyper-parameters which describe the physical behaviour of the air parcel movement. These hyper-parameters are: (i) the friction coefficient (α) which stands for the acceleration of the air parcel according to the gravity; (ii) the universal gas constant (g); (iii) the absolute temperature (T); and (iv) a constant (c) which equals negative value of 2 multiplied by R and T. The values of these hyper-parameters affect the accuracy of the results. Thus, these hyper-parameters must

be selected optimally. To do so, the CMAES is applied to optimize these hyper-parameters [25]. To improve the exploration and exploitation and to achieve a better balance between them in the classical WDO algorithm, the mutation is integrated. The mutation is used to improve the searching strategy to find the global optimum in the classical WDO algorithm.

The population of air parcels in the IWDO algorithm is randomly generated and distributed in random positions with random velocities in the searching space. The location and velocity for each air parcel are updated at each iteration using the mathematical model of the air parcels. In addition, the hyper-parameters are also updated using the CMAES, simultaneously. Accordingly, the IWDO generates a mutant vector with respect to each individual by integrating the mutation operation. The searching process in the IWDO algorithm is carried out based on six phases; initialization, pressure evaluation, CMAES, ranking of air parcel, mutation operation, best induvial comparison and selection and termination criterion. The pseudo-code of the IWDO algorithm is shown in Table 1.

Accordingly, the stages of the searching process in the IWDO algorithm are summarized as follows:

1) Initialization phase: Several parameters are initialized. These parameters are D_j, N_k which is the multiplication of D_j by 10, $Upper_j$, $Lower_j$, G_{max} and u_{max}. In this phase, the objective function is also defined which will be used to evaluate the pressure of the air parcels based on the limits for each D_j. According to all of the previously mentioned parameters, the $\overrightarrow{y_{NJ}^k}$ and $\overrightarrow{u_{NJ}^k}$ for each air parcel are generated randomly.
2) Pressure evaluation phase: At each iteration, the defined objective function is utilized to evaluate the pressure value for each air parcel separately. Based on the pressure evaluation, the population limits are scaled within the range of [-1, 1] as [4]:

$$x_j^k = \left(Upper_j - Lower_j\right) \times \left(\left(\frac{y_j^k + 1}{2}\right) + Lower_j\right) \quad (8)$$

3) CMAES phase: In this phase, the CMAES is utilized to find the optimal values of the hyper-parameters at each iteration. The CMAES optimizes the hyper-parameters according to distribution of the air parcels population which is sampled by a standard deviation of one third of each parameter's range in the search space. The population of air parcels is reformed by reshaped Gaussian distributions based on the modified distributions at each iteration. The new distribution is defined a covariance matrix. Accordingly, the covariance matrix is updated, and the optimal shape of the distribution is determined. Based on that, the step size is also updated. This process is repeated at each iteration until the desired value of the objective function is achieved. More details about CMAES algorithm can be found in [30, 31].
4) Ranking of air parcel phase: The air parcels are sorted based on the best value of the objective function ~~descendinglyin~~ in descending order. After the descending order of the air parcels indices, the

velocity and position for each air parcel are updated towards the air parcel that has the best value of the objective function as [24]:

$$\overrightarrow{u^k_{new_j}} = (1-\alpha)u^k_{c_{j-1}} - g y^k_{c_{j-1}} + \left(\left|\frac{1}{r^k}\right| \times \left(y^k_{opt_j} - y^k_{c_{j-1}}\right) RT\right) + \left(\frac{c\overrightarrow{u_0}}{r^k}\right) \quad (9)$$

$$\overrightarrow{y^k_{new_j}} = y^k_{c_{j-1}} + \left(\overrightarrow{u^k_{new_j}} \times \Delta t\right) \quad (10)$$

where $\overrightarrow{u_0} = \theta \times \vec{u}$.

5) Mutation operation phase: The IWDO algorithm employs the mutation operation to enhance its exploration capability by generating $Vec_{i,G}$ with respect to each $Z_{i,G}$. For each $Z_{i,G}$ at G, the $Vec_{i,G}$ is generated by the DE/best/1 strategy as [28]:

$$\sum_{i=1}^{N_k} Vec_{i,G}(j) = Z_{best,G}(j) + F.\left(Z_{r^i_{1,G}}(j) - Z_{r^i_{2,G}}(j)\right) \quad (11)$$

The term λ is applied to control the exploitation and the exploration of the IWDO. The value of λ decreases from 1 to 0 as the iteration number is increased. Accordingly, the individuals start the explore process in the initial iteration, while performing exploitation as the number of iterations increases [27]. Meanwhile, λ is updated as follows:

$$\lambda = 1 - \frac{G}{G_{max}} \quad (12)$$

The mutation is applied in the IWDO algorithm due to its superior performance at exploring the search space [32]. Accordingly, the new position for jth individual in the next iteration lies between X_i and U_i. The position is selected based on the boundary constraints of the solutions. In case the constraints of the solutions are braked, the repairing rule is utilized by [27],

$$Z_{i,G}(j) = \begin{cases} \delta_j + rndreal(0,1) \times (\mu_j - \delta_j), & if\ Z_i(j) < \delta_j \\ \mu_j - rndreal(0,1) \times (\mu_j - \delta_j), & if\ Z_i(j) < \mu_j \end{cases} \quad (13)$$

6) Best individual comparison and selection phase: In this phase, the values of the objective functions which are obtained by the ranking of air parcel phase and mutation phase are evaluated and compared. Accordingly, the selection phase is applied as [28]:

$$Z_{best,G}(j) = \begin{cases} U_G(j), & if\ f(U_G(j) < f(Z_G(j))) \\ Z_G(j), & Otherwise \end{cases} \quad (14)$$

7) Termination criterion: The IWDO algorithm will repeat the steps 2-6 until satisfying the termination criterion. The termination criterion for finding the global ~~opima~~optima will be satisfied by reaching the maximum iterations number.

4. Proposed method

The proposed method to identify the nine unknown parameters in a triple-diode PV cell model is summarized in Figure 2.

The proposed method can be categorized into six stages to identify the unknown parameters for each PV module. These stages are categorized as follows:

Stage 1: *Import the actual data, set the parameters of the optimization problem and define the objective function*:

The actual recorded data for each PV module are imported in this stage, which includes solar radiation, ambient temperature and the I-V pairs. The G_{max} and the N_k are set. Then, the maximum and minimum boundaries for each parameter (I_{Ph}, I_{0_1}, I_{0_2}, I_{0_3}, a_1, a_2, a_3, R_s and R_{sh}) are set. Next, the objective function is defined and utilized to evaluate the identified parameters to obtain the global optimal values. Here, the objective function is defined in the form of RMSE as in Eq. (5) and Eq. (6).

Stage 2: *Define the search space for each photovoltaic technology:*

In this stage, the search space is set to identify the unknown parameters for each PV module according to N. Therefore, the proposed method is run for each PV module separately for N iterations.

Stage 3: *Apply the proposed algorithm to identify the unknown parameters:*

The proposed IWDO algorithm, which is illustrated in Table 1, is implemented for identifying the unknown parameters for each PV module. The proposed algorithm aims to identify the unknown parameters from each I-V curve in each PV module based on the defined objective function. The identified parameters are reused to obtain the I-V curves using the Newton-Raphson method and then compared with the actual one. The result of this comparison aims to minimize the value of the RMSE. Accordingly, the identified parameters that have a minimum value for the objective function are stored and considered as the optimal values. This stage is repeated until reaching the maximum value of N for each PV module.

Stage 4: *Generalize the identified parameters for each photovoltaic technology:*

For each PV module, N number of each parameter is defined. Therefore, a matrix $9\times N$ of the identified parameters is obtained. This matrix should be generalized to find one value for each of the nine identified parameters. In this paper, the normal average (NAvg) model is used. This model is the arithmetic mean. The NAvg value for each parameter is calculated by dividing the summation of all the identified values for each parameter over the number of these values which equals to N. The mathematical formula of the NAvg can be represented as [26]:

$$NAvg = \frac{1}{N}\sum_{i=1}^{N} Parameter_i \tag{15}$$

In addition, the standard deviation (SD) is obtained to quantify the amount of variation for each of the generalized value. The SD is given by,

$$SD = \sqrt{\frac{1}{M-1}\sum_{i=1}^{M}(Parameter_i - \overline{Parameter})^2} \quad (16)$$

Stage 5: *Compare the identified parameters by the proposed algorithm with other existing algorithms:*

The accuracy of identified parameters using the IWDO algorithm are validated by comparing them with those obtained by other existing algorithms. This comparison is carried out based on some performance metrics. In this paper, the normalized root-mean-square error (nRMSE), mean absolute percentage error (MAPE), and coefficient of determination (R^2) are utilized. The nRMSE, MAPE and R^2 can be mathematically formulated as:

$$nRMSE = \frac{\sqrt{\frac{1}{N}\sum_{i=1}^{N}\left(I_{c_i} - I_{a_i}\right)^2}}{mean(I_a)} \quad (17)$$

$$MAPE = \frac{100}{N}\sum_{i=1}^{N}\left|\frac{I_{c_i} - I_{a_i}}{I_a}\right| \quad (18)$$

$$R^2 = 1 - \frac{Var(I_c - I_a)}{Var(I_a)} \quad (19)$$

Moreover, the convergence speed is used in the comparison to show the required convergence time for each algorithm to obtain the global optimal parameters.

Stage 6: *Display the optimal parameters, their generalized values and the performance metrices:*

The optimal identified nine parameters are displayed in this stage as well as the generalized value for each parameter with its standard deviation and the values of the nRMSE, MAPE, and R^2 for each PV module using the proposed algorithm and the other existing algorithms.

5. Simulation Results and Discussion

To verify the efficacy of the developed model which is named as the IWDO algorithm in identifying the nine unknown parameters in a triple-diode PV cell model, three PV technologies are used, namely, mono-crystalline, poly-crystalline and thin-film technologies. In this paper, the used PV modules are: a mono-crystalline LG300N1C-A3 (M1) PV module, poly-crystalline JAP6-60-250W/3BB (M2) PV module, and thin-film Avancis PowerMax smart 125W (M3) PV module. The proposed algorithm is applied in the aforementioned PV modules to identify their unknown parameters based on actual recorded data. The performance of the proposed model is compared with those obtained by several recent algorithms under different environmental conditions to prove its effectiveness.

5.1. Data

In this paper, actual recorded data based on 15 minutes intervals for 3 years are used. The dataset was recorded by the Commonwealth Scientific and Industrial Research Organisation (CSIRO), New South Wales (NSW), Australia (Latitude: -32.883889, Longitude: 151.728889) at a 30º tilt angle and a 0 º

azimuth angle. The size of the dataset for M1, M2 and M3 is 44749, 67416 and 56379 I-V characteristic curves, respectively. Accordingly, each I-V characteristic curve for M1 and M2 contains 28 I-V pairs, while M3 contains 29 I-V pairs.

The dataset may contain several spikes and non-stationary samples because of the uncertainty. These samples are known as outliers' points which may affect negatively on the accuracy of the obtained results. Therefore, an outlier measure is used to detect, remove and replace any point that that majorly deviates from the trend in each dataset. Here, the expected outliers in the dataset are shown in Figure 3 which is represented as a percentage of outliers in each pattern for each PV module.

In Figure 3, the datasets for M1, M2 and M3 are categorized to 6 patterns. From Figure 3.a, the outlier points in each pattern in the dataset of M1 from 1 to 6 are 5.33%, 3.01%, 1.99%, 0.98%, 4.22% and 2.71%, respectively. While, the outlier points in each pattern in the dataset of M2 from 1 to 6 are 1.09%, 5.01%, 2.99%, 6.12%, 3.11% and 1.92%, respectively. Finally, the outlier points in each pattern in the dataset of M3 from 1 to 6 are 3.99%, 0.98%, 1.98%, 6.11%, 5.22% and 2.81%, respectively. It is noticed that the outliers are only a few points in each dataset for M1, M2 and M3, however they negatively impact its performance. In this paper, the density-based spatial clustering of applications with noise (DBSCAN) algorithm is applied in the dataset to remove and replace them [26].

5.2. Simulation setup

The experimental setup is carried out according to Figure 2. As there are three PV modules, the proposed method is run 3 times separately for 44749, 67416 and 56379 iterations for M1, M2 and M3 PV modules, respectively. The experimental setup starts by importing the pre-processed data for each PV module. Several parameters are set in this stage. Here, the dimensions of the optimization problem are assigned to be 9, which represents the number of the unknown parameters in a triple-diode PV cell model. Accordingly, the population size is set to be 90. Next, the maximum number of iterations is set to 500. The aim of the objective function is to minimize the value of the RMSE between the calculated and actual I-V pairs. The calculated I-V pairs are estimated using the Newton-Raphson method based on the identified parameters. Each dimension represents one of the unknown parameters which has a certain research space. Based on the literature, the bounds for each parameter are set as follow: (i) in the range of [1,8] A for I_{Ph}; (ii) in the range of [1E-12,1E-5] A for I_{0_1}, I_{0_2} and I_{0_3}; (iii) in the range of [1,5] for a_1, a_2 and a_3; (iv) in the range of [0.1,2] Ω for R_s; and (v) in the range of [100,5000] Ω for R_{sh}.

Here, the IWDO algorithm is used to identify the unknown parameters based on the actual I-V characteristic curve as explained in Table 1. The parameters that have a minimum value of RMSE are selected as desired identified parameters for the triple-diode PV cell model. To test the effectiveness of the IWDO, the generated I-V characteristic curves based on the identified parameters of the M1, M2 and M3 PV modules are illustrated in Figure 4 in reference to the actual I-V characteristic curves.

From Figure 4, the average values of the nRMSE in Figure 4.a, Figure 4.b and Figure 4.c are 0.0374%, 0.3869% and 0.9812%, respectively. Finally, the average values of the nRMSE, MAPE, R^2 and the convergence speed in M3 are 0.0407%, 01223%, 99.1521% and 9.2210 s., respectively. Thus, it can be noticed that the generated I-V characteristic curves in Figure 4 are significantly closer to the experimental I-V characteristic curves with a negligible error, which shows the effectiveness of the proposed model.

5.3. Comparison and validation

In this paper, all the identifying algorithms were carried out in MATLAB 2019b environment which was run using a Windows 10 operating system in a standard PC with a 3.4 GHz Intel(R) Core (TM) i7-6700 CPU and 16 GB of RAM. The IWDO algorithm as well as WDO, AWDO, MFO [7], SFO [13] and IOWO [6] algorithms are used to identify the unknown parameters in the triple-diode PV cell model. As is mentioned above, each dataset contains a certain number of I-V characteristic curves, then as set of parameters are identified for each of these I-V characteristic curves. To generalize these parameters, the NAvg model is used. Accordingly, the generalized obtained parameters for M1, M2 and M3 are reported in Table 2.

The difference of the rate of convergence~~y speed~~ of the average fitness function values of the SFO, MFO, IOWO, WDO, AWDO and IWDO models under various weather conditions for M1, M2 and M3 PV modules are illustrated in Figure 5.

Based on Figure 5, the IWDO model converges faster than the aforementioned algorithms for M1, M2 and M3 PV modules. Here, the convergence speed of the proposed model is faster by 10.0951 s., 13.9842 s., 5.6283 s., 10.4977 s. and 10.8684 s. in M1, while it is faster by 13.0007 s., 12.1013 s., 6.9905 s., 10.9702 s. and 11.2456 s. in M2 and it is faster by 14.1111 s., 17.1111 s., 10.1111 s., 13.2837 s. and 13.6470 s. in M3 than that resulted using SFO, MFO, IOWO, WDO and AWDO models, respectively. Therefore, the proposed model has better convergence toward the global optimum in terms of accuracy and convergence time than the other models.

In order to verify the superiority of the proposed model, its performance is compared with that obtained by other algorithms based on nRMSE, MAPE and R^2 as well as the convergence speed. The minimum, maximum and average values of the nRMSE, MAPE, R^2 and the convergence speed of the proposed model as well as the other models are listed in Table 3.

From Table 3, it is clear that the proposed model outperforms the other benchmark models with respect to accuracy and convergence speed. Here, the average fitness function of the proposed algorithm is less by about 98.23%, 99.07%, 69.37%, 98.81% and 98.22% in M1, 90.81%, 82.05%, 58.04%, 88.74% and 81.37% in M2, and 96.02%, 97.95%, 80.76%, 96.43% and 88.65% in M3 than that obtained by SFO, MFO, IOWO, WDO and AWDO algorithms, respectively. In addition, the value of the average SD for the M1, M2 and M3 PV modules based on the proposed model are less than that resulted by the

aforementioned models which verifies the effectiveness of the proposed model. The average nRMSE value of the proposed model for all the PV models is less than that obtained by the benchmark models. In addition, the proposed model has better results than the other models in terms of MAPE and R^2. Those express the high accuracy of the obtained results by the proposed model. Finally, the proposed model is faster than the other models in terms of the average convergence speed.

6. Conclusion

This paper proposed and validated an improved wind driven optimization (IWDO) algorithm to identify the nine unknown parameters in a triple-diode PV cell model. The triple-diode PV cell model expressed the non-linearity between the meteorological variables and the current components including the effect of the grain boundaries, the carrier recombination and the leakage current is investigated. The triple-diode PV cell model has been demonstrated using the I-V curves. The IWDO algorithm utilizes the mutation strategy of DE algorithm and covariance matrix adaptation evolution strategy (CMAES) to enhance the exploration and the searching ability of the classical WDO algorithm. Three of commercial PV modules (LG300N1C-A3, JAP6-60-250W/3BB and Avancis PowerMax smart) are utilized to show the effectiveness of the proposed model.

The accuracy of the proposed model is validated internally by comparing the actual I-V curves with the generated I-V curves based on the identified parameters for each PV technology. In addition, an external validation is also carried out between the proposed model and the WDO, AWDO, MFO, SFO and IOWO algorithms. This comparison is conducted in terms of statistical error terms and the convergence speed. The average values of the SD, nRMSE, MAPE and R^2 of the proposed model are better than those obtained by the aforementioned models. Moreover, the proposed model is faster than the benchmark models in terms of the convergence speed. Accordingly, the average values of the nRMSE, MAPE, R^2 and the convergence speed of the proposed model in M1 are 0.0374%, 0.6332% and 99.1261% and 12.2270 s., respectively. While, the average values of the nRMSE, MAPE, R^2 and the convergence speed in M2 are 0.3869%, 0.9812%, 99.02112% and 10.2208 s., respectively. Finally, the average values of the nRMSE, MAPE, R^2 and the convergence speed in M3 are 0.0407%, 01223%, 99.1521% and 9.2210 s., respectively. Therefore, the IWDO algorithm outperforms the WDO, AWDO, MFO, SFO and IOWO algorithms in terms of nRMSE, MAPE, R^2 and the convergence speed.

To sum up, the ability of the proposed algorithm is improved in finding the global optimum of the identified parameters with better accuracy and convergence speed comparing with the aforementioned algorithms under any operating condition based on 15-minute intervals. Therefore, the IWDO algorithm is recommended to identify the triple-diode PV cell model's parameters.

References

[1] Chen X, Yu K. Hybridizing cuckoo search algorithm with biogeography-based optimization for estimating photovoltaic model parameters. Sol Energy 2019;180:192–206.

https://doi.org/10.1016/j.solener.2019.01.025.

[2] Jadli U, Thakur P, Shukla RD. A new parameter estimation method of solar photovoltaic. IEEE J Photovoltaics 2018;8:239–47. https://doi.org/10.1109/JPHOTOV.2017.2767602.

[3] Cardenas AA, Carrasco M, Mancilla-David F, Street A, Cardenas R. Experimental Parameter Extraction in the Single-Diode Photovoltaic Model via a Reduced-Space Search. IEEE Trans Ind Electron 2017;64:1468–76. https://doi.org/10.1109/TIE.2016.2615590.

[4] Mathew D, Rani C, Rajesh Kumar M, Wang Y, Binns R, Busawon K. Wind-Driven Optimization Technique for Estimation of Solar Photovoltaic Parameters. IEEE J Photovoltaics 2018;8:248–56. https://doi.org/10.1109/JPHOTOV.2017.2769000.

[5] Kassis A, Saad M. Analysis of multi-crystalline silicon solar cells at low illumination levels using a modified two-diode model. Sol Energy Mater Sol Cells 2010;94:2108–12. https://doi.org/10.1016/j.solmat.2010.06.036.

[6] Abd Elaziz M, Oliva D. Parameter estimation of solar cells diode models by an improved opposition-based whale optimization algorithm. Energy Convers Manag 2018;171:1843–59. https://doi.org/10.1016/j.enconman.2018.05.062.

[7] Allam D, Yousri DA, Eteiba MB. Parameters extraction of the three diode model for the multi-crystalline solar cell/module using Moth-Flame Optimization Algorithm. Energy Convers Manag 2016;123:535–48. https://doi.org/10.1016/j.enconman.2016.06.052.

[8] Tong NT, Pora W. A parameter extraction technique exploiting intrinsic properties of solar cells. Appl Energy 2016;176:104–15. https://doi.org/10.1016/j.apenergy.2016.05.064.

[9] Waly HM, Azazi HZ, Osheba DSM, El-Sabbe AE. Parameters extraction of photovoltaic sources based on experimental data. IET Renew Power Gener 2019;13:1466–73. https://doi.org/10.1049/iet-rpg.2018.5418.

[10] Pillai DS, Rajasekar N. Metaheuristic algorithms for PV parameter identification: A comprehensive review with an application to threshold setting for fault detection in PV systems. Renew Sustain Energy Rev 2018;82:3503–25. https://doi.org/10.1016/j.rser.2017.10.107.

[11] Abbassi R, Abbassi A, Jemli M, Chebbi S. Identification of unknown parameters of solar cell models: A comprehensive overview of available approaches. Renew Sustain Energy Rev 2018;90:453–74. https://doi.org/10.1016/j.rser.2018.03.011.

[12] Khanna V, Das BK, Bisht D, Vandana, Singh PK. A three diode model for industrial solar cells and estimation of solar cell parameters using PSO algorithm. Renew Energy 2015;78:105–13. https://doi.org/10.1016/j.renene.2014.12.072.

[13] Qais MH, Hasanien HM, Alghuwainem S. Identification of electrical parameters for three-diode photovoltaic model using analytical and sunflower optimization algorithm. Appl Energy 2019;250:109–17. https://doi.org/10.1016/j.apenergy.2019.05.013.

[14] Jordehi AR. Parameter estimation of solar photovoltaic (PV) cells: A review. Renew Sustain Energy Rev 2016;61:354–71. https://doi.org/10.1016/j.rser.2016.03.049.

[15] Huang W, Jiang C, Xue L, Song D. Extracting solar cell model parameters based on chaos particle swarm algorithm. 2011 Int Conf Electr Inf Control Eng ICEICE 2011 - Proc 2011:398–402. https://doi.org/10.1109/ICEICE.2011.5777246.

[16] Rezaee Jordehi A. Enhanced leader particle swarm optimisation (ELPSO): An efficient algorithm for parameter estimation of photovoltaic (PV) cells and modules. Sol Energy 2018;159:78–87. https://doi.org/10.1016/j.solener.2017.10.063.

[17] Jordehi AR. Time varying acceleration coefficients particle swarm optimisation (TVACPSO): A new optimisation algorithm for estimating parameters of PV cells and modules. Energy

Convers Manag 2016;129:262–74. https://doi.org/10.1016/j.enconman.2016.09.085.

[18] Merchaoui M, Sakly A, Mimouni MF. Particle swarm optimisation with adaptive mutation strategy for photovoltaic solar cell/module parameter extraction. Energy Convers Manag 2018;175:151–63. https://doi.org/10.1016/j.enconman.2018.08.081.

[19] Nunes HGG, Pombo JAN, Mariano SJPS, Calado MRA, Felippe de Souza JAM. A new high performance method for determining the parameters of PV cells and modules based on guaranteed convergence particle swarm optimization. Appl Energy 2018;211:774–91. https://doi.org/10.1016/j.apenergy.2017.11.078.

[20] Jamadi M, Merrikh-Bayat F, Bigdeli M. Very accurate parameter estimation of single- and double-diode solar cell models using a modified artificial bee colony algorithm. Int J Energy Environ Eng 2016;7:13–25. https://doi.org/10.1007/s40095-015-0198-5.

[21] Jiang LL, Maskell DL, Patra JC. Parameter estimation of solar cells and modules using an improved adaptive differential evolution algorithm. Appl Energy 2013;112:185–93. https://doi.org/10.1016/j.apenergy.2013.06.004.

[22] Niu Q, Zhang L, Li K. A biogeography-based optimization algorithm with mutation strategies for model parameter estimation of solar and fuel cells. Energy Convers Manag 2014;86:1173–85. https://doi.org/10.1016/j.enconman.2014.06.026.

[23] Chen X, Yu K, Du W, Zhao W, Liu G. Parameters identification of solar cell models using generalized oppositional teaching learning based optimization. Energy 2016;99:170–80. https://doi.org/10.1016/j.energy.2016.01.052.

[24] Bayraktar Z, Komurcu M, Werner DH. Wind Driven Optimization (WDO): A novel nature-inspired optimization algorithm and its application to electromagnetics. 2010 IEEE Antennas Propag. Soc. Int. Symp., 2010. https://doi.org/10.1109/APS.2010.5562213.

[25] Bayraktar Z, Komurcu M, Werner DH. Adaptive Wind Driven Optimization. Proc. 9th EAI Int. Conf. Bio-inspired Inf. Commun. Technol. (formerly BIONETICS), Belgium: ACM; 2016. https://doi.org/10.4108/eai.3-12-2015.2262424.

[26] Ibrahim IA, Hossain MJ, Duck BC, Fell CJ. An Adaptive Wind-Driven Optimization Algorithm for Extracting the Parameters of a Single-Diode PV Cell Model. IEEE Trans Sustain Energy 2020;11:1054–66. https://doi.org/10.1109/TSTE.2019.2917513.

[27] Mostafa Bozorgi S, Yazdani S. IWOA: An improved whale optimization algorithm for optimization problems. J Comput Des Eng 2019;6:243–59. https://doi.org/10.1016/j.jcde.2019.02.002.

[28] Wang C, Liu Y, Liang X, Guo H, Chen Y, Zhao Y. Self-adaptive differential evolution algorithm with hybrid mutation operator for parameters identification of PMSM. Soft Comput 2018;22:1263–85. https://doi.org/10.1007/s00500-016-2413-6.

[29] Bayraktar Z, Komurcu M, Bossard JA, Werner DH. The wind driven optimization technique and its application in electromagnetics. IEEE Trans Antennas Propag 2013;61:2745–57. https://doi.org/10.1109/TAP.2013.2238654.

[30] Hansen N, Ostermeier A. Adaptive arbitrary normal mutation distribution in evolution strategies: The covariance matrix adaptation. Proc. IEEE Int. Conf. Evol. Comput., 1996, p. 312–7. https://doi.org/10.1109/ICEC.1996.542381.

[31] Gregory MD, Bayraktar Z, Werner DH. Fast optimization of electromagnetic design problems using the covariance matrix adaptation evolutionary strategy. IEEE Trans Antennas Propag 2011;59:1275–85. https://doi.org/10.1109/TAP.2011.2109350.

[32] Gong W, Cai Z, Ling CX. DE/BBO: A hybrid differential evolution with biogeography-based

518 optimization for global numerical optimization. Soft Comput 2011;15:645–65.
519 https://doi.org/10.1007/s00500-010-0591-1.

520

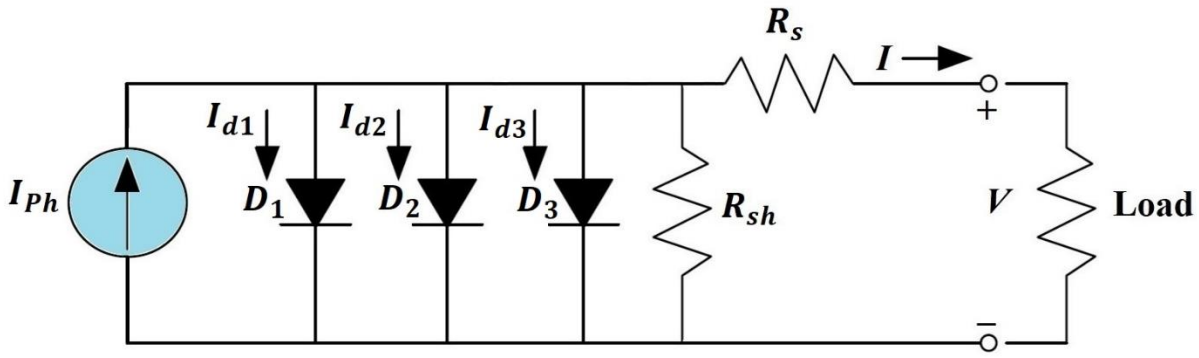

Figure 1. The electrical equivalent circuit for a triple-diode PV cell model

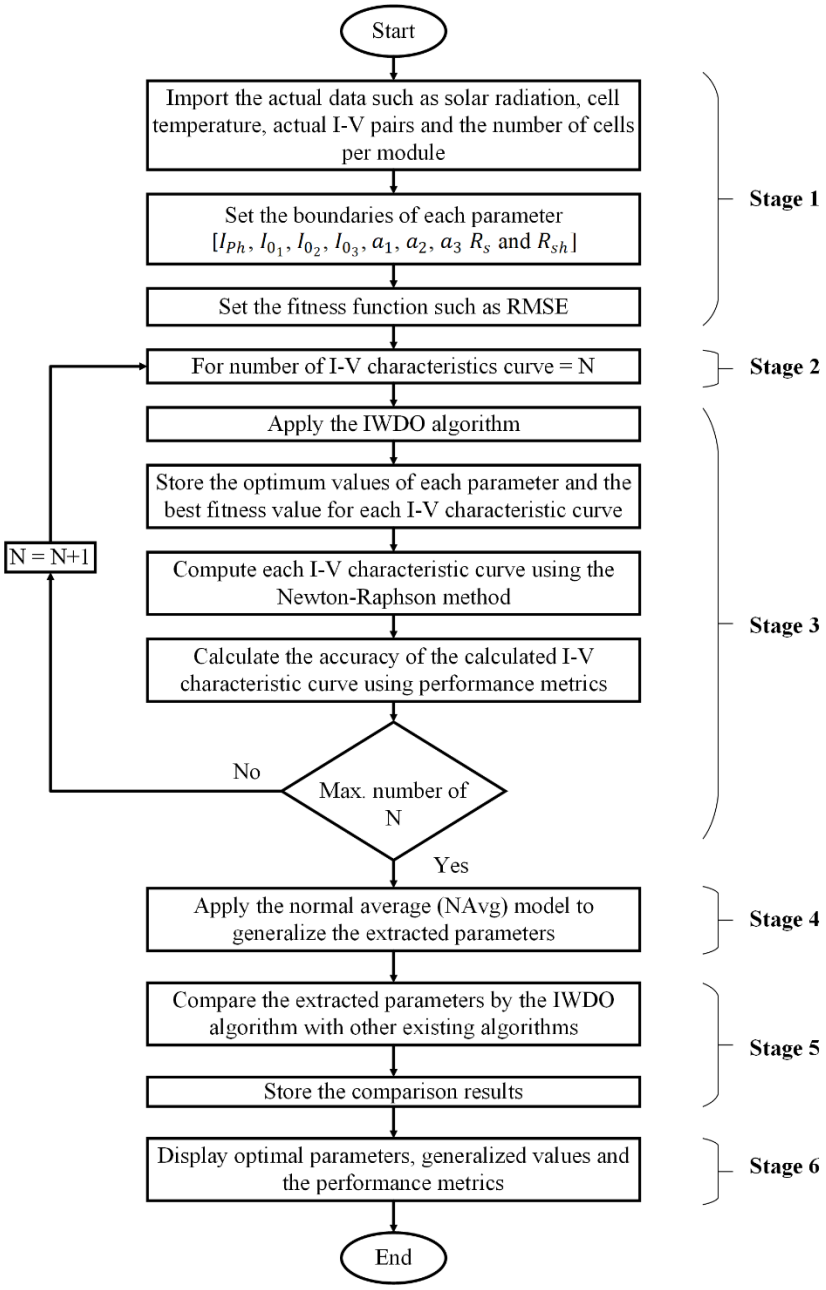

Figure 2. The flowchart of the proposed unknown parameters identification method in a triple-diode PV cell model

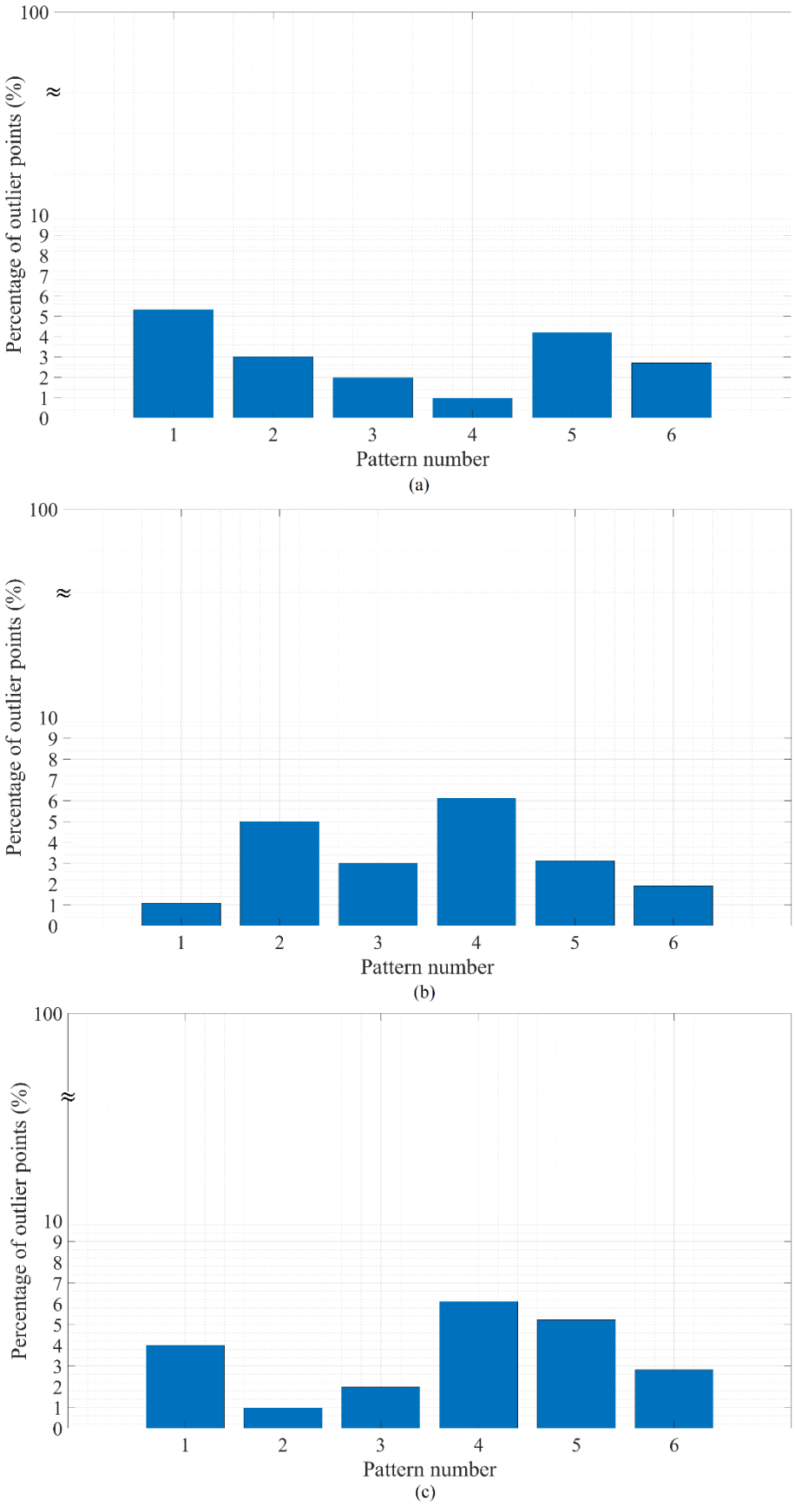

Figure 3. Outlier measures in the datasets of the M1, M2 and M3 PV modules: (a) LG300N1C-A3 (M1), (b) JAP6-60-250W/3BB (M2) and (c) Avancis PowerMax smart 125W (M3)

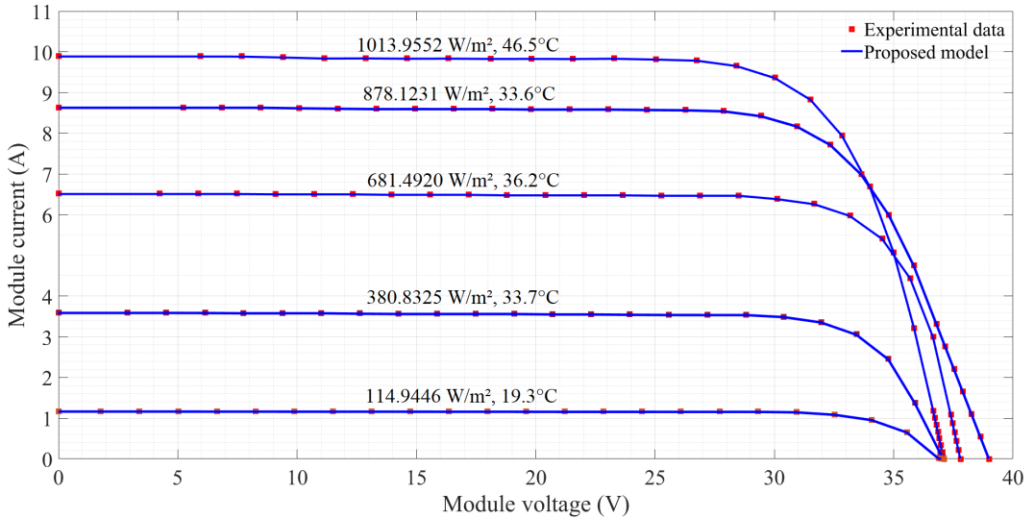

(a)

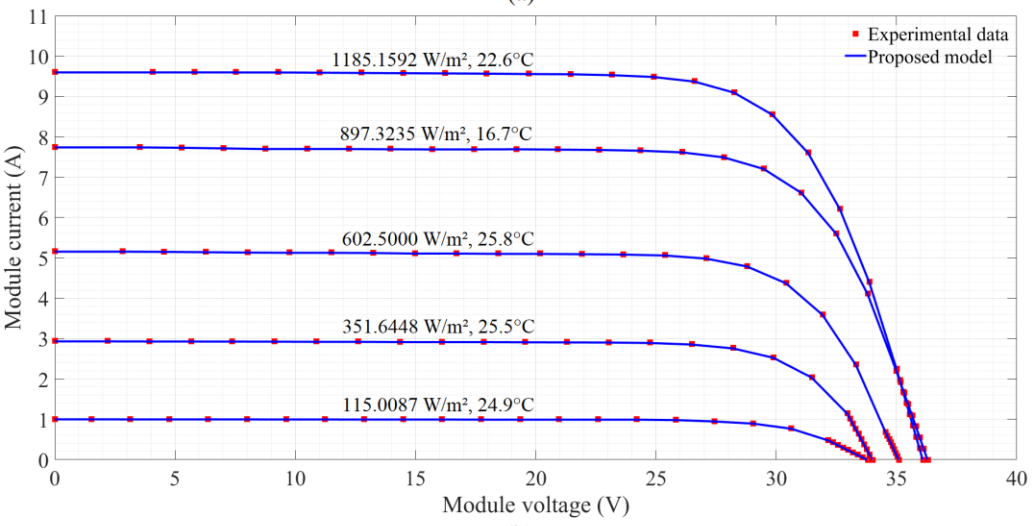

(b)

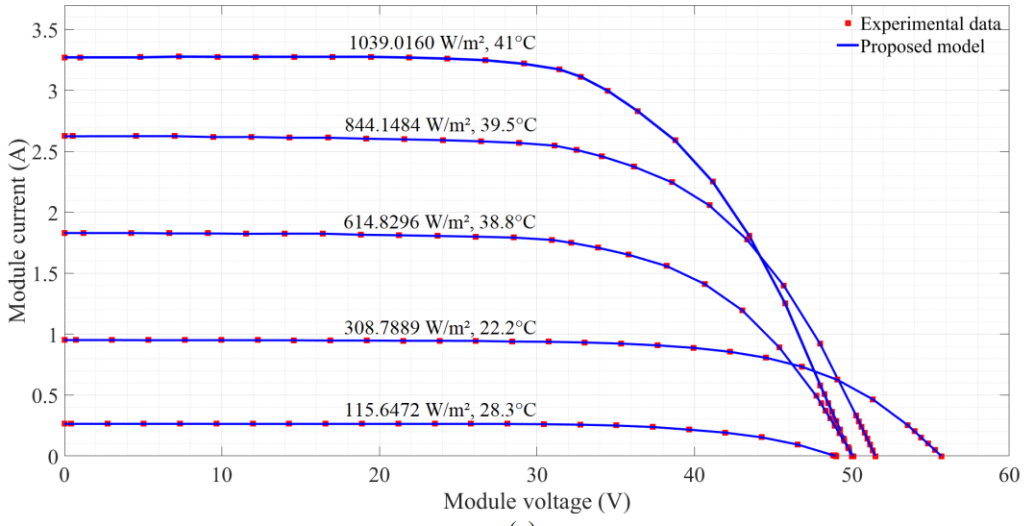

(c)

Figure 4. Experimental and computed I-V characteristic curves of the M1, M2 and M3 PV modules using the IWDO model under various weather conditions: (a) I-V characteristic curves of LG300N1C-A3 (M1), (b) I-V characteristic curves of JAP6-60-250W/3BB (M2) and (c) I-V characteristic curves of Avancis PowerMax smart 125W (M3)

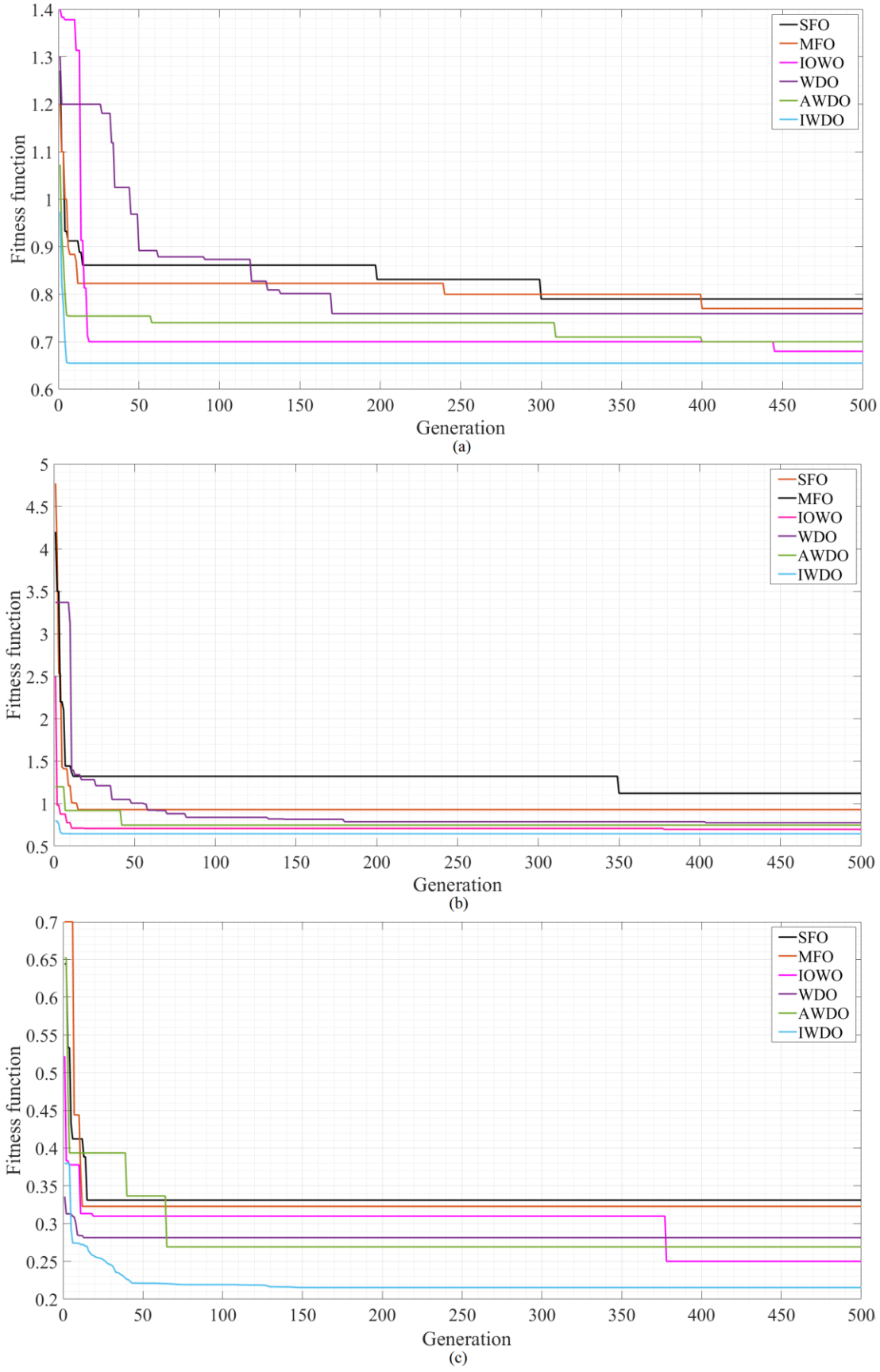

Figure 5. Development of the average fitness function values of SFO, MFO, IOWO, WDO, AWDO and IWDO models to identify the nine unknown parameters: (a) M1, (b) M2 and (c) M3

567 Table 1. Pseudo code of the Improved wind driven optimization (IWDO) algorithm

1: **Begin**
2: Generate the initial population, $x_j^d \epsilon[-1,1]$, where $j = 1, 2, \ldots, N_k$ and $d = 1, 2, \ldots, D_j$
3: Randomize the initial values of α, g, c and RT
4: Evaluate the fitness function for each air parcel in x_j^d
5: Obtain the minimum value of the fitness function, $P_0 = f_{min}$
6: Set $Z^* = P_0$
7: **while** The termination criterion in not satisfied **do**
8: Rank the values of the fitness function for each air parcel descendingly
9: **for all** i **do**
10: Update $p = rndreal(0,1)$ and $\lambda = 1 - (G/G_{max})$
11: Calculate j_{rand}, $j_{rand} = rndint(1, n)$
12: **for all** j **do**
13: **if** $p < \lambda$ **then**
14: Update the velocity by Eq. (9)
15: Check velocity limits
16: Update air parcel positions by Eq. (10)
17: Call CMAES
18: Return the new values of α, g, c and RT
19: Evaluate the new solution
20: Update $P(i,j)$
21: **if** $P(i,j) < P_0$ **then**
22: $global_P = P(i,j)$
23: **end if**
24: Find the global optimum (x_{global})
25: Set $X_i^* = x_{global}$
26: **else**
27: Select uniform randomly $r_1 \neq r_2 \neq r_3 \neq i$
28: **if** $\lambda \leq 0.5$ **then**
29: $U_i^*(j) = Z_i^*(j) + F \times \left(Z_{r_1}(j) - Z_{r_2}(j)\right)$
30: **else**
31: Re-select $r_1 \neq r_2 \neq r_3 \neq i$
32: $U_i^*(j) = Z_i^*(j) + F$
33: **end if**
34: **end if**
35: **end for**
36: **if** U_i^* is better than X_i^* **then**
37: Update best individual, $X_i^* = U_i^*$
38: **end if**
39: Return the values of the best individual and f_{min}
40: **end for**
41: $G = G + 1$
42: **end while**
43: **End**

568

569

570

571

572 Table 2. Comparison of the identified unknown parameters for the selected PV modules by various evolutionary models under different operating conditions

Parameter	Model	X_1			..	X_n			NAvg		
		M1	M2	M3	..	M1	M2	M3	**M1**	**M2**	**M3**
I_{Ph} (A)	SFO [14]	4.4451	4.3981	2.1545	..	4.7128	4.5091	1.9832	**4.5331**	**4.4556**	**2.2210**
	MFO [7]	4.7312	4.6712	2.9931	..	4.4456	4.4891	3.2114	**4.5551**	**4.4495**	**3.2019**
	IOWO [6]	4.2591	4.7124	1.4678	..	4.4412	4.1446	1.7634	**4.2301**	**4.2551**	**1.8440**
	WDO	4.5984	4.6712	4.6289	..	4.6821	4.5291	4.5671	**4.5405**	**4.5352**	**4.6237**
	AWDO	4.4986	4.7661	1.9251	..	4.6124	4.4561	1.9783	**4.5250**	**4.6700**	**1.8434**
	IWDO*	4.0912	4.1981	1.9832	..	4.5913	4.5612	1.7655	**4.1696**	**4.2776**	**1.7114**
I_{0_1} (A)	SFO [14]	4.6009E-6	4.8221E-6	5.1082E-6	..	4.6612E-6	4.6771E-6	4.9881E-6	**4.6112E-6**	**4.7850E-6**	**5.0019E-6**
	MFO [7]	4.0988E-6	3.0991E-6	5.9908E-6	..	4.3009E-6	3.2100E-6	6.2012E-6	**4.3351E-6**	**3.1125E-6**	**6.3325E-6**
	IOWO [6]	4.6606E-6	4.7987E-6	5.0100E-6	..	4.5765E-6	4.9801E-6	5.5618E-6	**4.6629E-6**	**4.8851E-6**	**5.3329E-6**
	WDO	5.0092E-6	4.9982E-6	4.9808E-6	..	5.2109E-6	5.1123E-6	5.0125E-6	**5.0268E-6**	**5.0386E-6**	**5.1191E-6**
	AWDO	2.2272E-6	2.1198E-6	9.0992E-6	..	2.4873E-6	2.0189E-6	9.2067E-6	**2.3644E-6**	**2.1358E-6**	**9.1968E-6**
	IWDO*	4.7721E-6	4.8791E-6	5.2981E-6	..	4.6886E-6	5.0912E-6	5.5092E-6	**4.7413E-6**	**4.9011E-6**	**5.4920E-6**
I_{0_2} (A)	SFO [14]	4.5918E-6	4.6916E-6	5.6295E-6	..	4.7778E-6	4.7009E-6	5.7882E-6	**4.6012E-6**	**4.7215E-6**	**5.6631E-6**
	MFO [7]	4.0937E-6	3.1973E-6	6.2990E-6	..	4.2915E-6	3.3908E-6	6.6008E-6	**4.1102E-6**	**3.2982E-6**	**6.5651E-6**
	IOWO [6]	4.4511E-6	4.7718E-6	5.0094E-6	..	4.6218E-6	4.9891E-6	5.2202E-6	**4.5510E-6**	**4.8099E-6**	**5.0112E-6**
	WDO	4.8920E-6	4.9912E-6	4.9981E-6	..	5.0016E-6	5.1910E-6	5.2007E-6	**5.0274E-6**	**5.0392E-6**	**5.1172E-6**
	AWDO	2.5018E-6	2.0900E-6	9.1094E-6	..	2.4661E-6	2.1971E-6	9.0898E-6	**2.3452E-6**	**2.0986E-6**	**9.1837E-6**
	IWDO*	4.5601E-6	4.8709E-6	5.3992E-6	..	4.7210E-6	4.9981E-6	5.5055E-6	**4.7554E-6**	**4.8913E-6**	**5.4956E-6**
I_{0_3} (A)	SFO [14]	4.6124E-6	4.3127E-6	5.7220E-6	..	4.4418E-6	4.5127E-6	5.5509E-6	**4.5245E-6**	**4.4211E-6**	**5.5501E-6**
	MFO [7]	4.1273E-6	3.9981E-6	5.9998E-6	..	3.9812E-6	4.0091E-6	6.1198E-6	**4.1121E-6**	**3.9981E-6**	**6.2211E-6**
	IOWO [6]	4.6512E-6	4.5561E-6	5.2095E-6	..	4.6123E-6	4.7128E-6	5.0091E-6	**4.4451E-6**	**4.6651E-6**	**5.1121E-6**
	WDO	5.0092E-6	5.1224E-6	5.2612E-6	..	5.1092E-6	4.8991E-6	5.0992E-6	**5.0280E-6**	**5.0384E-6**	**5.1148E-6**
	AWDO	2.4123E-6	2.0213E-6	9.2091E-6	..	2.5092E-6	2.2289E-6	9.3912E-6	**2.3875E-6**	**2.1204E-6**	**9.2110E-6**
	IWDO*	4.7123E-6	4.6651E-6	5.5239E-6	..	4.6699E-6	4.9712E-6	5.3441E-6	**4.7347E-6**	**4.8733E-6**	**5.4900E-6**
a_1	SFO [14]	3.2115	3.3212	4.0981	..	2.9981	3.2114	4.4123	**3.0112**	**3.1121**	**4.1001**
	MFO [7]	3.6214	4.1234	4.5981	..	3.8123	3.7891	4.1982	**3.5561**	**3.8810**	**4.2991**
	IOWO [6]	2.9771	2.8991	4.1082	..	2.8776	3.2351	4.3981	**2.8991**	**2.9921**	**4.1121**
	WDO	3.2124	3.1259	2.9899	..	2.9981	2.9981	3.1258	**3.0244**	**3.0255**	**3.0288**
	AWDO	3.4891	3.6812	4.4561	..	3.9812	3.9781	4.4179	**3.7153**	**3.8471**	**4.3170**
	IWDO*	2.9981	2.9821	3.8569	..	2.8871	2.7761	4.2309	**2.9067**	**2.9224**	**4.0773**
a_2	SFO [14]	3.3451	3.1230	4.2346	..	3.3321	3.1081	4.3226	**3.2210**	**3.0049**	**4.2119**
	MFO [7]	3.5712	4.0117	4.1892	..	3.5312	4.1812	4.4981	**3.4889**	**3.9901**	**4.2215**
	IOWO [6]	2.8712	3.0192	3.9981	..	2.7981	2.8991	4.4271	**2.7998**	**2.9011**	**4.1992**

	WDO	3.1530	3.1451	3.2145	..	2.9812	3.1231	2.9812	**3.0229**	**3.0252**	**3.0299**
	AWDO	3.5761	3.8991	4.2598	..	3.6081	3.7891	4.5312	**3.6943**	**3.8418**	**4.3155**
	IWDO*	2.8981	3.0812	4.0912	..	2.7612	2.7812	4.1762	**2.9042**	**2.9196**	**4.0784**
a_3	SFO [14]	3.2291	2.9812	4.0912	..	3.2122	2.7781	4.2123	**3.1991**	**2.8991**	**4.1009**
	MFO [7]	3.2114	3.8912	3.8913	..	3.1889	3.7116	4.0921	**3.2113**	**3.7811**	**3.9881**
	IOWO [6]	2.4998	3.1224	3.7881	..	2.7771	2.9881	4.0121	**2.6891**	**3.0112**	**3.8991**
	WDO	3.1298	3.0112	3.0192	..	2.8991	2.8891	2.9889	**3.0225**	**3.0238**	**3.0273**
	AWDO	3.5778	3.7881	4.2151	..	3.6781	3.9881	4.4412	**3.7164**	**3.8407**	**4.3157**
	IWDO*	2.9981	2.9912	3.9889	..	2.7719	2.7881	4.1992	**2.8971**	**2.8971**	**4.0802**
R_s (Ω)	SFO [14]	1.9212	1.8892	1.9821	..	1.9872	2.0912	1.7182	**1.8112**	**1.9221**	**1.7881**
	MFO [7]	1.4512	1.6092	1.2988	..	1.5612	1.4256	1.4112	**1.4112**	**1.5125**	**1.3811**
	IOWO [6]	1.2998	1.2981	1.5091	..	1.4123	1.3387	1.6123	**1.1221**	**1.3888**	**1.4551**
	WDO	1.0789	1.1227	1.1098	..	1.0889	1.0089	1.0521	**1.0277**	**1.0274**	**1.0673**
	AWDO	1.8891	2.0781	2.0012	..	2.0991	1.9881	1.8912	**1.8584**	**1.9310**	**1.9511**
	IWDO*	1.0078	1.5762	1.7882	..	1.0221	1.3981	1.6781	**1.0006**	**1.4922**	**1.6969**
R_{sh} (Ω)	SFO [14]	2822.1982	2886.9802	459.8712	..	2890.2126	2889.9811	460.1982	**2813.2231**	**2889.2163**	**455.1150**
	MFO [7]	2440.0091	2666.8212	2779.9821	..	2451.9821	2667.9802	2781.2981	**2445.6223**	**2665.5512**	**2788.1562**
	IOWO [6]	2251.0218	2360.9821	1118.7211	..	2259.0901	2359.8720	1122.0921	**2258.2231**	**2355.1556**	**1120.2113**
	WDO	2560.0780	2566.2098	2658.9889	..	2555.0921	2567.8750	2622.9882	**2556.2604**	**2560.5961**	**2612.0580**
	AWDO	2844.0867	2977.0670	340.0877	..	2809.8088	2975.8912	345.9762	**2831.0188**	**2973.2236**	**344.6717**
	IWDO*	2258.7001	1189.0097	1199.0091	..	2266.0668	1199.7609	1188.9811	**2260.1132**	**2251.6297**	**1191.7816**

*IWDO is the proposed model.

n represents the last sample in the database which equals 44749, 67416 and 56379 for M1, M2 and M3, respectively.

582 Table 3. Performance comparison for several evolutionary parameters' identification models

Performance index	M1						M2						M3					
	SFO [13]	MFO [7]	IOWO [6]	WDO	AWDO	IWDO*	SFO [13]	MFO [7]	IOWO [6]	WDO	AWDO	IWDO*	SFO [13]	MFO [7]	IOWO [6]	WDO	AWDO	IWDO*
Standard deviation	7.2331E-8	2.4110E-7	2.1221E-8	2.8190E-7	6.5600E-8	**1.7511E-8**	1.8995E-7	3.2210E-7	1.2155E-7	3.3370E-7	1.5970E-7	**1.0080E-7**	3.2215E-8	5.5449E-8	1.2159E-8	6.4321E-8	1.4245E-8	**0.3290E-8**
Min. nRMSE (%)	0.9885	1.0001	0.6221	1.0748	**0.4612**	0.5348	0.7552	1.2201	0.4551	1.1318	0.7344	**0.2049**	0.0811	0.5221	0.0991	0.1738	0.0851	**0.0029**
Max. nRMSE (%)	4.3351	5.6612	**1.1221**	6.5600	6.6645	1.5655	7.5512	8.2251	2.5112	7.1484	8.9419	**2.2675**	5.1121	5.2114	1.2219	4.8009	5.1485	**0.9647**
Avg. nRMSE (%)	2.1125	4.0155	0.1221	3.1549	2.1016	**0.0374**	4.2112	2.1559	0.9221	3.4347	2.0772	**0.3869**	1.0221	1.9821	0.2115	1.1405	0.3586	**0.0407**
Min. MAPE (%)	1.2212	1.4221	0.9223	1.5663	1.1123	**0.0112**	1.1120	2.9221	0.7221	1.2210	0.9921	**0.2112**	1.0220	1.5221	0.1221	1.1223	0.9221	**0.0912**
Max. MAPE (%)	3.2112	2.3651	1.3152	2.2213	1.5213	**1.0221**	3.2215	5.2215	2.1251	3.2115	1.2215	**0.9221**	3.5962	4.6215	1.5593	4.2513	3.2225	**1.0002**
Avg. MAPE (%)	2.1221	1.9251	1.1123	1.8922	1.3221	**0.6332**	2.1221	3.2541	1.1223	2.0292	1.0226	**0.9812**	1.8213	3.2111	1.1251	2.6221	1.8951	**0.1223**
Min. R^2 (%)	95.5515	91.2251	94.5512	93.2112	95.2121	**96.2315**	94.9521	93.0015	96.6612	94.3321	95.1252	**97.1251**	93.0215	93.0085	94.9952	92.0021	93.3221	**95.3662**
Max. R^2 (%)	97.2151	96.0215	98.3623	96.1225	98.0221	**99.9915**	97.2152	97.6155	98.3251	98.8512	97.8512	**99.2151**	98.1125	97.9882	99.2151	98.0215	98.9225	**99.5622**
Avg. R^2 (%)	97.0215	95.8512	96.5120	95.3212	96.3251	**99.1261**	96.9851	97.0021	97.2512	97.8991	97.1212	**99.0112**	97.9251	97.2151	98.9812	97.0515	98.1251	**99.1521**
Min. convergence speed (s.)	20.2212	23.5512	15.6332	20.6406	21.0156	**10.3361**	15.6651	20.1125	12.3301	13.9688	14.1406	**9.2210**	16.3321	19.3325	12.3365	17.7344	15.9688	**7.0229**
Max. convergence speed (s.)	37.2551	41.2263	31.2215	38.2656	40.0937	**28.1101**	36.3325	42.1152	27.5112	41.7500	37.9219	**22.2293**	40.3351	55.3215	25.3321	66.3125	42.8281	**15.3381**
Avg. convergence speed (s.)	22.3221	26.2112	17.8553	22.7247	23.0954	**12.2270**	23.2215	22.3221	17.2113	21.1910	21.4664	**10.2208**	23.3321	26.3321	19.3321	22.5047	22.8628	**9.2210**

583 *IWDO is the proposed model.